Virology 489 (2016) 95–107

Contents lists available at ScienceDirect

Virology

journal homepage: www.elsevier.com/locate/yviro

Peripheral effects induced in BALB/c mice infected with DENV by the intracerebral route

E.R.A. Oliveira [a,1], J.F.S. Amorim [a,1], M.V Paes [a], A.S. Azevedo [a], A.J.S. Gonçalves [a], S.M. Costa [a], M. Mantuano-Barradas [a], T.F. Póvoa [a], J. de Meis [b], C.A. Basílio-de-Oliveira [c], A.C.M.A. Nogueira [a], A.M.B. Alves [a,*]

[a] Laboratory of Biotechnology and Physiology of Viral Infections, Oswaldo Cruz Institute, Oswaldo Cruz Foundation, Rio de Janeiro, Brazil
[b] Laboratory on Thymus Research, Oswaldo Cruz Institute, Oswaldo Cruz Foundation, Rio de Janeiro, Brazil
[c] Pathological Anatomy, Hospital Gaffrée Guinle, Federal University from the State of Rio de Janeiro (UNIRIO), RJ, Brazil

ARTICLE INFO

Article history:
Received 23 June 2015
Returned to author for revisions
6 October 2015
Accepted 15 December 2015
Available online 31 December 2015

Keywords:
Dengue
Mouse model
Intracerebral infection
Immune response
Central nervous system

ABSTRACT

The lack of an immunocompetent animal model for dengue mimicking the disease in humans is a limitation for advances in this field. Inoculation by intracerebral route of neuroadapted dengue strains in mice is normally lethal and provides a straightforward readout parameter for vaccine testing. However, systemic effects of infection and the immune response elicited in this model remain poorly described. In the present work, BALB/c mice infected by the intracerebral route with neuroadapted DENV2 exhibited several evidences of systemic involvement. DENV-inoculated mice presented virus infective particles in the brain followed by viremia, especially in late stages of infection. Infection induced cellular and humoral responses, with presence of activated T cells in spleen and blood, lymphocyte infiltration and tissue damages in brain and liver, and an increase in serum levels of some pro-inflammatory cytokines. Data highlighted an interplay between the central nervous system commitment and peripheral effects under this experimental condition.

Introduction

Dengue is an acute systemic viral disease that represents an escalating public burden, nowadays considered as the most relevant arthropod-borne illness. The virus, concentrated among tropical and subtropical regions worldwide, is transmitted mainly by *Aedes* mosquitoes, which put at risk of infection approximately half of the world's population. It is estimated that 390 million people are infected with dengue annually, of which 96 million manifest the symptoms of the disease resulting in around 20 thousand deaths (Gubler, 2012; Bhatt et al., 2013). Dengue virus (DENV) circulates as four distinct serotypes (DENV1 to 4) and infections can be oligosymptomatic or result in a mild flu-like illness known as dengue fever (DF). Life-threatening forms of the disease, dengue hemorrhagic fever (DHF) and dengue shock syndrome (DSS), occur in a minority of DF cases and exhibit manifestations such as plasma leakage, thrombocytopenia and hemorrhage, which can evolve to hypovolemic shock (Martina et al., 2009; Chuansumrit and Chaiyaratana, 2014). In addition, complications of dengue affecting specific organs and systems, such as the brain, peripheral nerves, liver, lung and heart, have recently been reported (Carod-Artal et al., 2013; Póvoa et al., 2014; Berkowitz et al., 2015). As there are no effective antiviral alternatives or a vaccine available to control dengue virus infection, currently, the countermeasures rely basically on vector control, educational programs and symptomatic treatments.

The lack of an immunocompetent animal model that mimics all the human clinical aspects of dengue is recognized as a key obstacle to understand the disease immunity and also to develop a vaccine. This fact led the scientific community to use alternative animal approaches for dengue research, including mouse–human chimeras, immunocompromised mice or models using non-physiological infection routes (Yauch and Shresta, 2008). These experimental models are very useful for investigating the mechanisms involved in the disease, but its use for vaccine testing can have some restrictions, since these mice may respond differently from immunocompetent animals. An immunocompetent mouse approach in which a mouse brain adapted virus, original from New Guinea and Hawaii dengue outbreaks, is intracerebrally injected in animals (Sabin and Schlesinger, 1945) has been extensively used in anti-dengue vaccine evaluation (Porter et al., 1998; Valdés et al., 2009; Clements et al., 2010; Azevedo et al., 2011; Costa et al.; 2011). Nevertheless, based on symptoms generally observed in these mice (paralysis) and the inoculation route, this animal approach is sometimes described as

* Corresponding author.
E-mail address: ada@ioc.fiocruz.br (A.M.B. Alves).
[1] These authors contributed equally to this work.

http://dx.doi.org/10.1016/j.virol.2015.12.006
0042-6822/

non-relevant when considering vaccine testing (World Health Organization, 2013; Plummer and Shresta, 2014). However, in humans, even though neurological signs may be statistically underestimated by clinical evaluations during dengue outbreaks, several forms of central and peripheral nervous system impairments have been described in patients with dengue (Sumarmo et al., 1978; Row et al., 1996; Misra and Kalita, 2009). A meta-analytical study of 15 reports considering symptoms as restlessness, irritability, dizziness, drowsiness, stupor, coma or convulsion, revealed different levels of correlation between these neurological signs and DSS. Strong correlations of encephalopathy with DSS were detected in five studies from Thailand and in a summary of other seven case-control studies (Huy et al., 2013). Important neurological manifestations were also reported in many dengue fatal cases (Kho et al., 1981; Sumarmo et al., 1983; Chimelli et al., 1990; Miagostovich et al., 1997), what emphasizes a possible close connection between the central nervous system (CNS) dysfunction and patients with severe dengue.

Despite the historical application of the intracerebrally-inoculated immunocompetent mouse approach for anti-dengue vaccine testing, protection was measured basically by survival/morbidity endpoints. Little is known about other possible effects induced after an intracerebral (i.c.) inoculation with DENV, regarding systemic aspects and the elicited immune response. On this purpose and based on the importance of an immunocompetent environment to study DENV infection and the efficacy of vaccines, here we aimed to investigate more deeply BALB/c mice intracerebrally inoculated with the mouse brain adapted DENV2 NGC strain. Infective virus particles were detected in the brain of these animals as well as in the circulation, mainly in late stages of infection. Infection induced activation of $CD4^+$ and $CD8^+$ T cells, detected in spleen and blood samples. T cell infiltrates were also observed in the brain and liver, which correlated with tissue damages in these organs. In addition, humoral immune response was elicited with activation and production of dengue specific antibodies and animals exhibited increased serum levels of pro-inflammatory cytokines. Taken together, this report brought new aspects involving immunological features of the studied mouse model and highlighted an interplay between the CNS commitment and the peripheral effects under this experimental condition.

Results

Morbidity and mortality of BALB/c mice intracerebrally infected with DENV2

In the experimental mouse model using BALB/c animals inoculated by the i.c. route with 40 LD_{50} of a mouse-brain adapted DENV2 virus (NGC strain), we observed a high mortality rate (90%), with deaths occurring from the 7th to the 15th day after infection (d.a.i.) (Fig. 1A). All mock-injected mice survived the procedure (mock and virus-infected animal groups were significantly different, $p < 0.0001$). After that, we verified the relationship between the occurrence of deaths and morbidity manifestation, mainly hind leg paralysis and/or alteration of spinal cord. For this purpose, mortality curves were built considering deaths preceded or not by symptoms related to central nervous system (CNS) dysfunction. Morbidity were evaluated at least 16 h before deaths and we found that a subset of DENV-infected mice (54.7%) died after exhibiting signs of CNS dysfunction while another group (35.3%) succumbed without exhibiting any apparent clinical signs (Fig. 1B). In general, deaths preceded by clinical signs were broadly distributed in time course (from 8 to 15 d.a.i.), while deaths without morbidity were more concentrated in the early stages of infection (from 7 to 10 d.a.i.). Therefore, data suggest that even though there is an important component leading to death clearly associated with CNS commitment, lethality, in several cases, is not necessarily preceded by the observed neurologic dysfunctions.

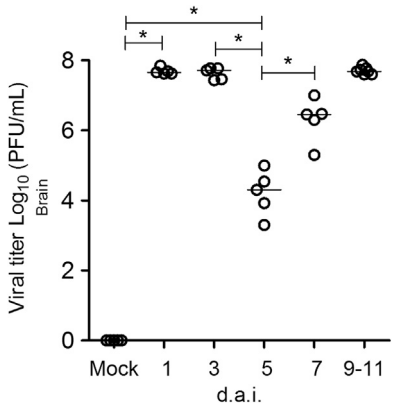

Fig. 2. Virus detection in brain samples collected from BALB/c mice infected with DENV2. Brain samples ($n=5$ to 7) extracted from mice at different days after infection were tested for the presence of infective virus particles as measured by indirect plaque assay in Vero cells. Virus titers are expressed by PFU count. Statistical differences were evaluated using Mann–Whitney test (*$p < 0.05$). d.a.i.-days after infection.

Table 1
Detection of virus in serum samples by qualitative analysis as evidenced by indirect plaque assay in Vero cells. Values represent the number of positive animals out of a total number of mice (between parentheses). d.a.i.-days after infection.

	d.a.i.					
	mock	1	3	5	7	9–11
Number of animals	0(5)	1(5)	2(5)	3(5)	2(5)	5(7)

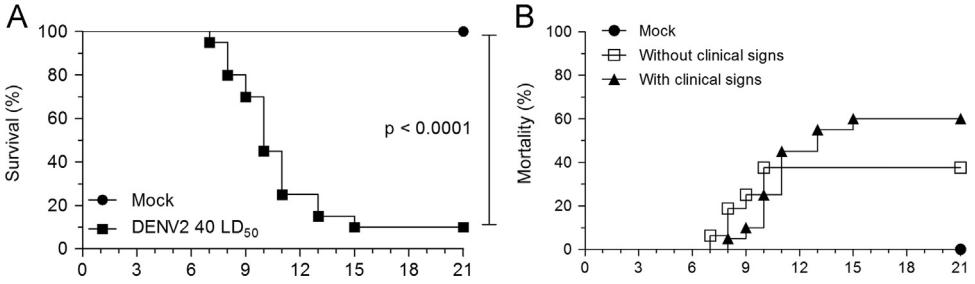

Fig. 1. Susceptibility of BALB/c mice to primary DENV infection by the i.c. route. BALB/c mice were intracerebrally inoculated with 40 LD_{50} of DENV2 NGC strain (DENV group) propagated in Vero cell cultures. Control group (Mock) is represented by animals injected with supernatants of non-infected Vero cell cultures. (A) Survival curves-mice were followed up for 21 days after infection. Kaplan–Meier distributions were compared using Log-Rank test using the mock group as a reference. (B) Mortality rates-Curves were built considering only deaths, preceded or not by CNS dysfunction, such as spinal cord alterations (hunchback posture) or paralysis observed at least 16 h before death. Data represent a compilation of three independent experiments with groups of 6 to 7 animals in each test ($n=20$). d.a.i.-days after infection.

Detection of DENV2-infective particles and virus antigen

The presence of infective DENV2 particles was investigated by plaque assay in Vero cell monolayers using brain, liver and serum samples from virus-inoculated BALB/c. All animals inoculated with DENV2 presented infective virus particles in the brain. Viral titers were significantly high throughout the entire evaluated period, although a decrease was observed in days 5 and 7 (Fig. 2). As expected, the control group (mock) showed no viral plaque formation.

Viremia was detected in animals infected with DENV2, yet in low magnitude and not in all serum samples (Table 1). The number of DENV2 positive serum samples gradually increased along the kinetic study. In the first day after infection, only one animal out of five showed viremia, while in the last tested points (9–11 d.a.i.) we observed five out of seven dengue positive serum samples. In order to ensure the virus spread in i.c.-inoculated mice, DENV2–NS3 antigen was stained by immunohistochemistry in liver samples collected from the 9th to the 11th d.a.i. As expected, controls (liver of mock-inoculated animals incubated with anti-NS3 antibody or the hepatic tissue of infected mice treated only with anti-rabbit IgG conjugate) did not present any positive reaction (Fig. 3a and b). On the other hand, the NS3 protein was detected in hepatocytes (Fig. 3c), Kupffer cells (Fig. 3d) and endothelial cells (Fig. 3e). The detection of NS3 not only endorsed the DENV spread in this murine model but also revealed virus replication in the liver. Therefore, in this murine model, the brain seemed to be the main organ for virus replication, although infection led to the spread of infective virus particles to the circulation reaching also a peripheral organ.

Activated T cells in spleen and blood

The levels of T cell populations and the presence of activated subpopulations were investigated in spleen and blood samples of DENV2-infected BALB/c mice. The flow cytometry gate strategy applied for this analysis is described in Fig. 4. No differences were detected on the percentages of $TCD4^+$ cells analyzed in splenocytes collected at all time points (1, 3, 5, 7 and 9–11 d.a.i.) when compared to non-infected controls (Fig. 5 top). Regarding the $TCD8^+$ subset, a percentage increase of this population was observed at the 5th d.a.i. and this effect remained throughout the rest of the experiment. We considered as a T cell activation marker the expression of $CD45RB^{low}$ on the cell surface. In this context, we found that percentages of both $TCD4^+CD45RB^{low}$ and $TCD8^+CD45RB^{low}$ splenocytes increased after DENV infection (Fig. 5 top). At the 3rd d.a.i., approximately 50% of $TCD4^+$ cells were $CD45RB^{low}$, whereas the activated $TCD8^+$ subpopulation, significantly detected only at the 5th d.a.i., represented about 20% of the $TCD8^+$ subset. When the same analysis was performed in blood samples, we observed a similar pattern. Percentages of $TCD4^+$ cells did not vary during the investigated period, while $TCD8^+$ subset was higher in day 5 when compared to non-infected samples (Fig. 5 bottom left). Concerning activated T lymphocytes, percentages of $TCD4^+CD45RB^{low}$ cells increased from day 3 onwards reaching a peak level at the 7th d.a.i. (about 40% of the $TCD4^+$), whereas the percentage of $TCD8^+CD45RB^{low}$ only increased significantly at the 5th d.a.i. (25% of the $TCD8^+$) (Fig. 5 bottom left). Levels of activated T cell subpopulations also increased significantly when analyzed by absolute counts (Fig. 5 bottom right). Negative control was performed using blood and spleen samples of mock-infected mice, measured at the 5th d.a.i., and no differences were found when compared to non-infected animals (day 0, data not shown). Taken together, results indicated that DENV infection by the i.c. route led to T cell activation.

T cell infiltrates and histopathological aspects of the brain of infected mice

Since the main clinical manifestations in this mouse model are related to CNS commitment, the presence of T cell infiltrates were

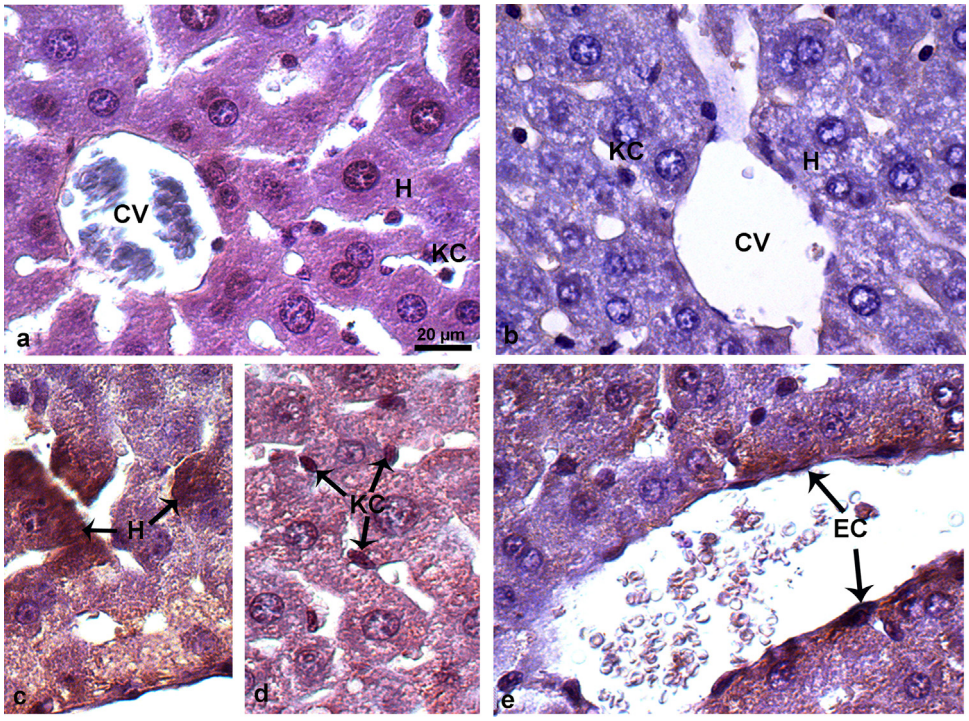

Fig. 3. Detection of NS3 protein in liver samples of BALB/c mice infected with DENV2. BALB/c mice were i.c.-inoculated with DENV2 NGC strain, sacrificed 10 d.a.i., and livers were processed for NS3 immunohistochemical staining. Liver of a mock-inoculated mouse incubated with anti-NS3 antibody and anti- rabbit IgG conjugate (a); Liver of a DENV2-infected mouse incubated only with anti-rabbit IgG conjugate (b); Liver tissue from an infected animal showing the detection of NS3 antigen in hepatocytes (c), Kupffer cells (d) and endothelial cells (e). Hepatocytes (H); Kupffer cells (KC); endothelial cells (EC). Arrows indicate positive reactions. Sections were counter stained with Harris hematoxylin. Image of infected mice is representative of positive animals found in viremia assay (Table 1, group 9–11 d.a.i.).

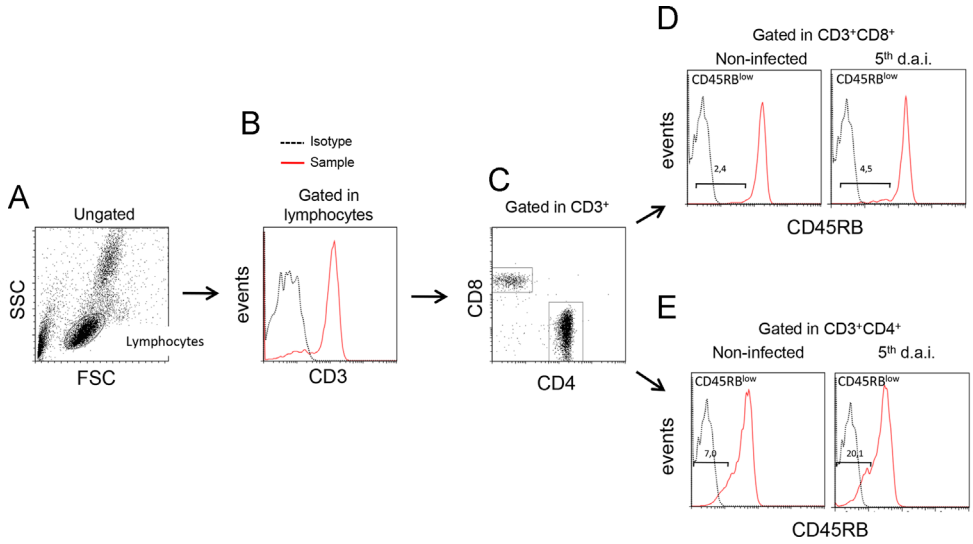

Fig. 4. Gate strategy for analysis of T cell activation in blood and spleen samples. (A) Ungated forward and side light scatter (FSC × SSC) dot plot exhibiting a region considered as the lymphocyte region. (B and C) Histograms showing the expression of CD4 and CD8 in the $CD3^+$ lymphocytes. (D and E) Histograms of representative blood samples (non-infected or 5 d.a.i.) exhibiting $CD45RB^{low}$ events (considered as activated T cells) measured in $CD3^+CD8^+$ or $CD3^+CD4^+$ counts. Values indicate percentages of cells. d.a.i.-days after infection.

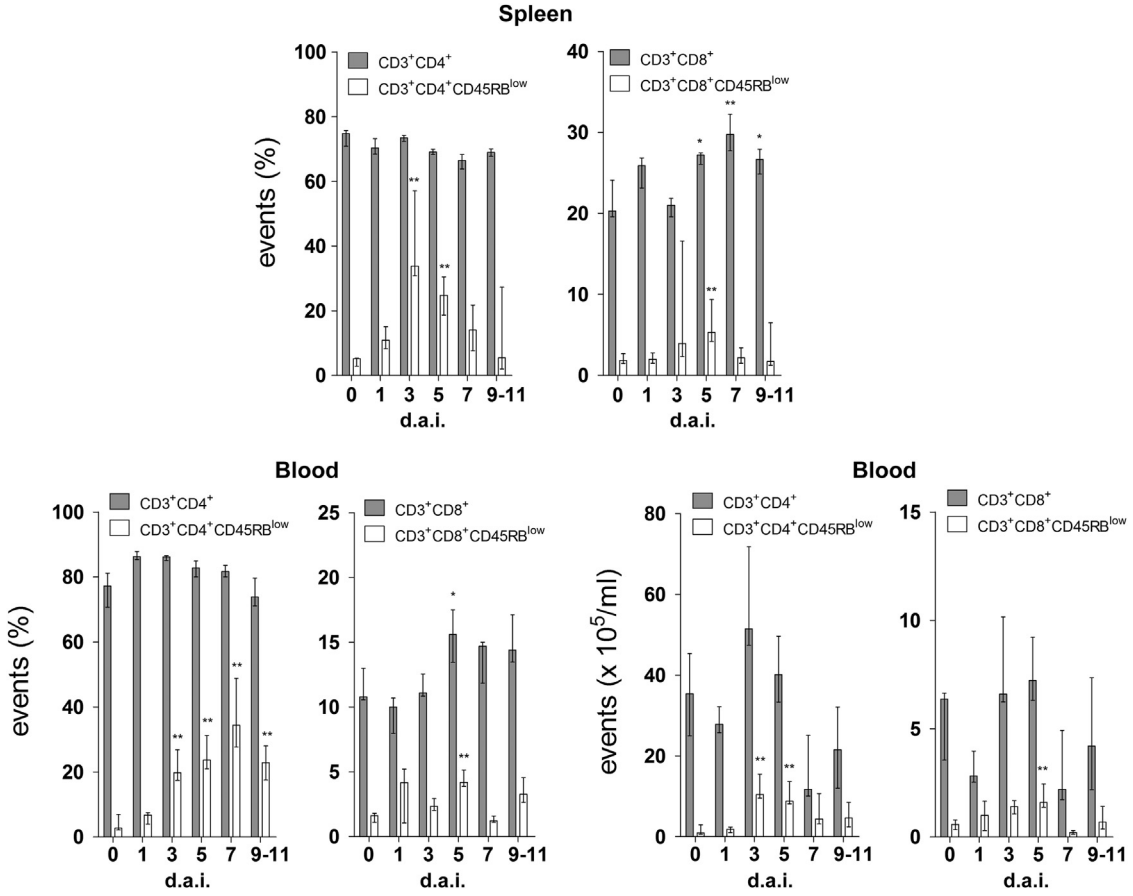

Fig. 5. T cell activation in spleen and blood of DENV-infected mice. The activation of T cells in mice infected with the mouse-brain adapted virus was studied based on the modulation of the expression of CD45RB on the lymphocyte surface. Spleen (top) and blood (bottom) samples were collected from BALB/c mice in different time points after infection with DENV2 and analyzed by flow cytometry. Activated cells ($CD45RB^{low}$) were measured in $CD3^+CD4^+$ or in $CD3^+CD8^+$ events, all gated in lymphocyte conventional region. Values represent percentages with median and interquartile range (top and bottom left). Absolute counts (bottom right) of T cells and activated subpopulations present in blood samples were measured in the time course of infection. Statistical differences between non-infected and infected groups were evaluated using Mann–Whitney test (*$p < 0.05$; **$p < 0.01$). Data represent a compilation of three independent experiments with groups of 5 animals in each test (total $n = 15$). d.a.i.-days after infection.

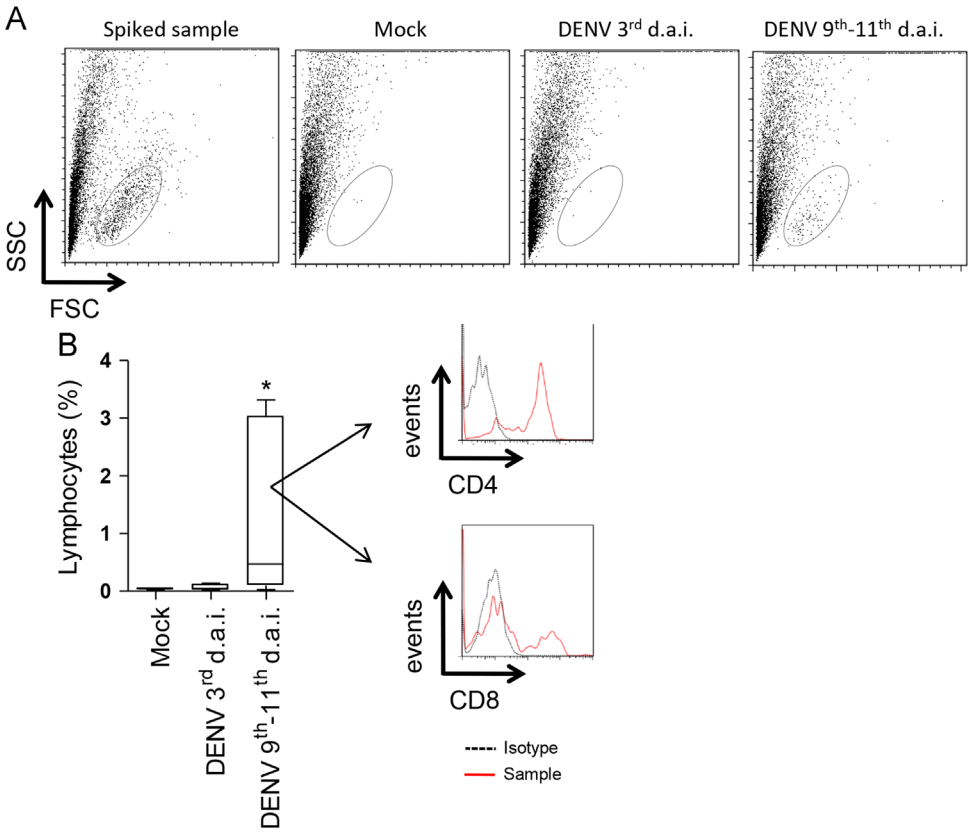

Fig. 6. Lymphocyte infiltrates into the brain of infected mice. (A) Original flow cytometry dot plots showing FSC × SSC of cells isolated from the brain of animals on days 3 and 9–11 after infection. An additional control consisted of a brain of non-infected mice, which was processed in the presence of a small portion of splenocytes obtained from the same animal (spiked sample), was performed in order to set the lymphocyte region for further analysis. (B) Percentages of lymphocytes present in samples of mock, 3 and 9–11 d.a.i. Histograms show the presence of $CD4^+$ and $CD8^+$ cells in the brain infiltrates. Statistical differences between mock and infected groups were evaluated using Mann–Whitney test ($^*p < 0.05$). Data represent a compilation of two independent experiments with groups of 5 animals in each test (total $n = 10$). d.a.i.-days after infection.

investigated in the brain of infected animals. For this purpose, animals on days 9 to 11 after infection with DENV2 (all of them showing clinical signs) were elected for this analysis and compared with early-infected (3rd d.a.i) and mock-infected mice. To ensure the feasibility of lymphocyte detection from brain samples by flow cytometry analysis, additional controls were made ("spiked sample"), in which brains from non-infected animals were macerated together with a small quantity of splenocytes obtained from the same animals. As indicated in Fig. 6A, splenocytes were successfully recovered from the spiked sample, thus confirming the usefulness of the applied protocol. After infection, a T cell population, including $CD4^+$ and $CD8^+$, was detected only in samples obtained at 9–11 days (Fig. 6A and B). In accordance to this observation, lymphocyte infiltrates were also seen in brain tissues of animals at the 10th d.a.i., as determined by histological analysis. In brain cuts, we observed diffuse mononuclear cell infiltrates in pia mater and molecular layer, as well as perivascular leukocyte cell migration inside interstitial temporal cortex (Fig. 7b and c). Interstitial hemorrhage was an additional alteration detected in brain tissues of infected mice (Fig. 7d). All together, both analyses showed that, in the present mouse model, severe symptomatic manifestations and T cell infiltrates in the brain occur simultaneously and may be somehow related.

T cell infiltrates detected in the liver and the commitment of this organ during infection

Besides studies concerning T cell infiltrates in the brain of infected mice, we also investigated the presence of lymphocyte infiltrates in the liver of these animals. Although mice were virus challenged by the i.c. route, the liver was evaluated since this organ is considered as an important target in dengue disease. Flow cytometry analysis was carried out according to Fig. 8. A significant increase on the percentages of $TCD8^+$ lymphocytes was detected in animals at 9–11th d.a.i., when compared to non-infected controls, while no differences on the percentages of $TCD4^+$ population were detected (Fig. 9 top). On the other hand, once considering activated ($CD45RB^{low}$) and effector ($CD44^{hi}CD62L^-$) subpopulations, we observed an increase in both $CD4^+$ and $CD8^+$ cells during the same period when compared to controls. The percentage of the $TCD8^+CD44^{hi}CD62L^-$ subpopulation was already increased at the 3rd d.a.i. (Fig. 9 bottom). These data were supported by histological findings, in which hepatic tissues of infected animals presented lymphocyte infiltrates either around the portal space or distributed in parenchyma, mainly in late stages of infection (Fig. 10d and e). Microsteatosis, necrosis and circulatory dysfunctions, such as hemorrhage and edema, were also characterized in interstitial parenchyma since the beginning of infection (one day after virus inoculation) (Fig. 10b and c). As expected, in control mice (mock-infected) the hepatic tissue exhibited regular and preserved structures (Fig. 10a). Consistent with histopathological observations, serum levels of AST significantly increased in mice after 9–11 d.a.i. (Fig. 11). After all, these data indicated that the liver was affected in the present mouse model, thus confirming that the virus infection by the i.c. route can evolve to a systemic commitment.

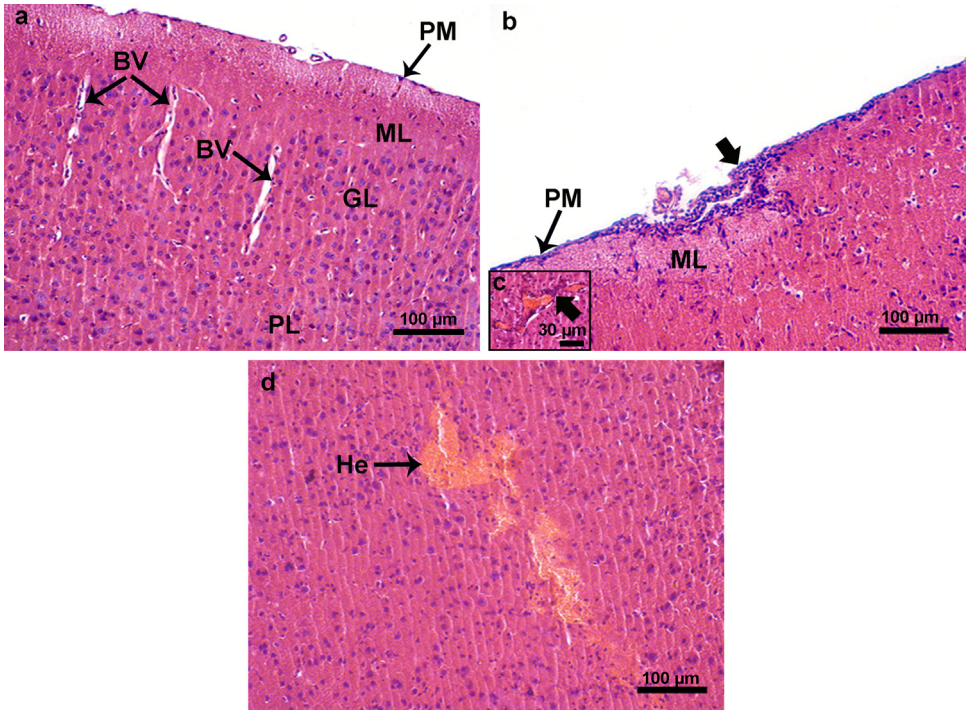

Fig. 7. Histopathological aspects of the brain tissue of BALB/c mice infected with DENV2. (a) A representative mouse inoculated with mock, revealing normal aspects of the cerebral cortex. (b) Animals infected with DENV2 showing mononuclear cell infiltrates (large black arrows) in pia mater and molecular layer. Commitment with perivascular leukocyte cell migration inside interstitial temporal cortex (c), and hemorrhage in the cerebral parenchyma (d), observed 10 days after infection. BV-Blood vessels; He-hemorrhage; PM-pia mater; ML-molecular layer, GL- granular layer, PL – piramidal layer. Tissue sections were stained with hematoxylin/eosin and visualized by optical microscopy.

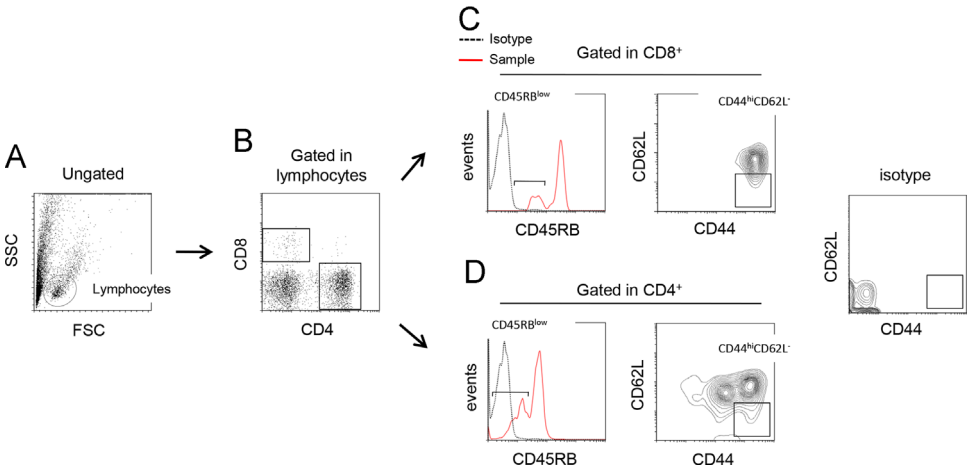

Fig. 8. Gate strategy for analysis of T cell activation in liver samples. Lymphocytes were isolated from liver by density gradient and analyzed by flow cytometry to investigate the presence of activated/effector T cells. (A) Ungated FSC × SSC flow cytometry dot plot exhibiting a region considered as the lymphocyte region. (B) Cytometric dot plot showing the $CD4^+$ and $CD8^+$ cells measured in the lymphocyte region. (C and D) Histograms and contour representations containing the considered regions of activated ($CD45RB^{low}$) or effector ($CD44^{hi}CD62L^-$) T cells measured in $CD8^+$ or $CD4^+$ counts isolated from an infected animal 10 days after infection.

B cell response in DENV infected mice

In order to investigate the participation of the host humoral immune response during infection, we first analyzed the expression of IgD in the surface of $B220^+$ cells using flow cytometry. Populations of higher ($B220^+_{hg}$) or lower ($B220^+_{lg}$) internal complexity, as determined by side scatter parameter (SSC), were analyzed separately since this phenotypic parameter can reflect an increase of synthesis and activation of cells (Fig. 12A). In this approach, we measured the down regulation of IgD on the surface of these cells, as an evidence of B cell differentiation. We observed, in blood and spleen samples, that DENV infection led to an increase of $B220^+_{hg}IgD^-$ cell percentages in late stages of the kinetic study (9–11 d.a.i.), when compared to controls (Fig. 12B and C). No differences were observed considering the $B220^+_{lg}IgD^-$ percentages between mock and infected groups (data not shown). ELISA assays using DENV2 NS1 as a solid-phase antigen were additionally performed in order to investigate the antibody secreting cell response against this virus protein. Consistent with the flow cytometry experiments described above, anti-NS1 IgM antibodies were detected at the 5th d.a.i., reaching titers of 1/200 in the final points of the study (9–11th d.a.i.). Anti-NS1 IgG

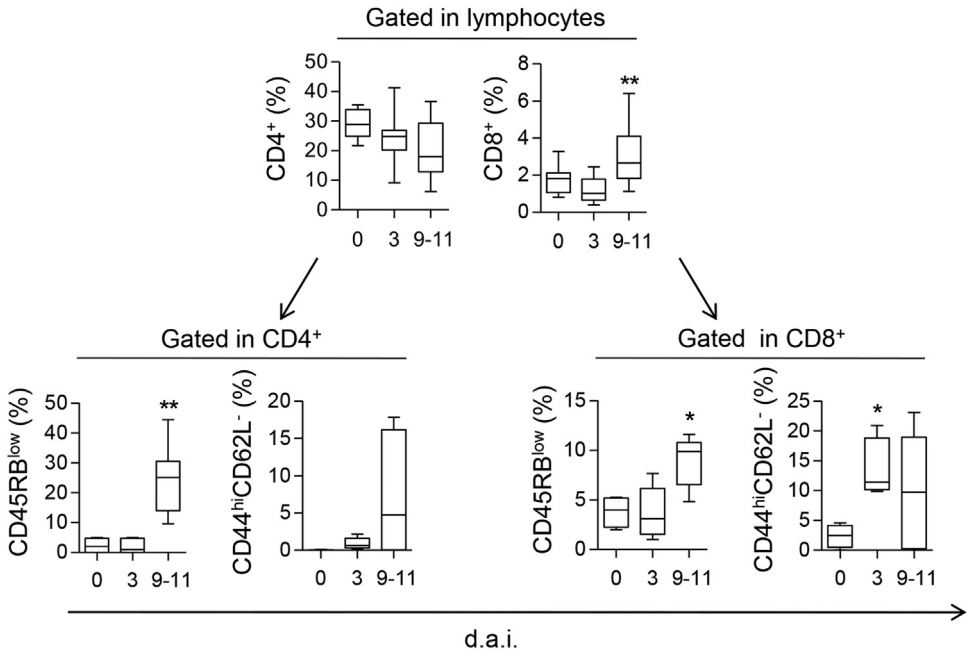

Fig. 9. Effector T cell response in the liver of infected mice. Effector T cell response was evaluated in the liver of BALB/c mice ($n=5$ per group) inoculated with DENV2 by the i.c. route in different days after infection. Flow cytometry analysis of samples isolated from the hepatic tissue, regarding T cell populations measured in the lymphocyte region (top: $CD4^+$ and $CD8^+$), and activated/effector T cell subpopulations measured in $CD4^+$ or $CD8^+$ events (bottom: $CD45RB^{low}$ and $CD44^{hi}CD62L^-$). Statistical differences between non-infected and infected groups were evaluated using Mann–Whitney test ($^*p<0.05$; $^{**}p<0.01$). Data represent a compilation of three independent experiments with groups of 5 animals in each test (total $n=15$). d.a.i.-days after infection.

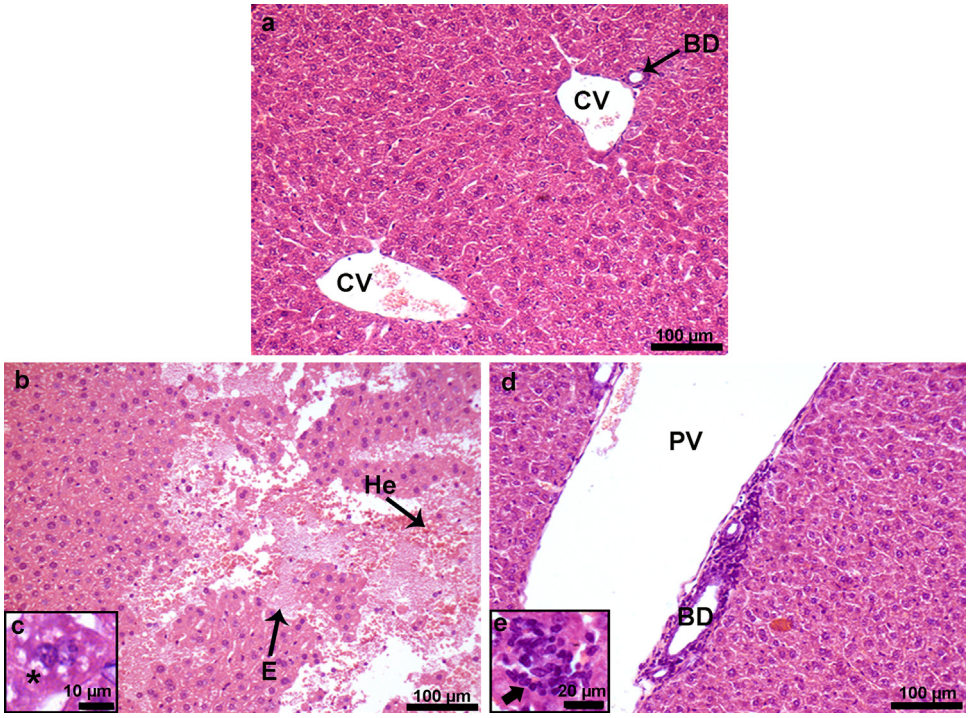

Fig. 10. Histopathological aspects of the liver tissue in BALB/c mice infected with DENV2. (a) A representative mouse inoculated with mock, revealing normal aspect of the hepatic parenchyma. (b–c) Animals infected with DENV2 exhibiting tissue damages, mainly edema, hemorrhage (b), necrosis and microesteatose (c) were already found in the beginning of infection (at the 1st and 5th d.a.i., respectively). Mononuclear infiltrates around the portal space (d) and distributed in the liver parenchyma (e) were observed 10 days post infection. CV-central vein; PV-portal vein; BD- biliar duct; E-edema; He-hemorrhage; Ne – necrosis; arrowhead indicate microesteatose; large black arrows indicate infiltrates. The tissue sections were stained with hematoxylin/eosin and visualized under optical microscopy.

antibodies were observed only in late stages of infection with titers of approximately 1/700 (Fig. 12D). Thus, results indicated the participation of the humoral immunity in response to DENV infection by the i.c. route, with activation of B lymphocytes and production of antibodies.

Pro-inflammatory cytokines present in blood of infected BALB/c mice

After showing the participation of T and B cell response elicited by the i.c. infection, the quantification of pro-inflammatory cytokines in blood was our next step to characterize this mouse model.

Plasma samples were extracted from DENV-infected animals and tested for IL-12p70, TNF-α, IFN-γ, MCP-1, IL-10 and IL-6 by cytometric bead array (CBA) technique. Following 24 h of virus challenge, levels of IL-12p70, TNF-α and MCP-1 significantly increased when compared to non-infected controls. Levels of all these cytokines dropped below limits of detection in the next evaluated days, but IL-12p70 and TNF-α increased again at the 7th d.a.i. (Fig. 13). Although levels of IL-10 and IL-6 were mostly beneath the detection limits, IL-10 showed a behavior similar to IL-12p70 and TNF-α, exhibiting peaks at days 1 and 7 after infection. Regarding IFN-γ, a significant peak was detected at the 7th d.a.i. Additional cytokine determinations were also performed in an attempt to correlate the serum levels with clinical manifestations in mice. Since the 7th day was the initial point where symptoms appeared, serum samples from 7–11 d.a.i. were analyzed and groups were divided as "with" or "without" clinical manifestations. Despite this effort, no statistical difference in cytokine levels was found between these studied groups (Fig S1). In a brief conclusion, the cytokine profiles suggested activation of innate mechanism at the beginning of infection, followed by an induction of the adaptive immunity, as seen by the INF-γ increase at late stages of the study.

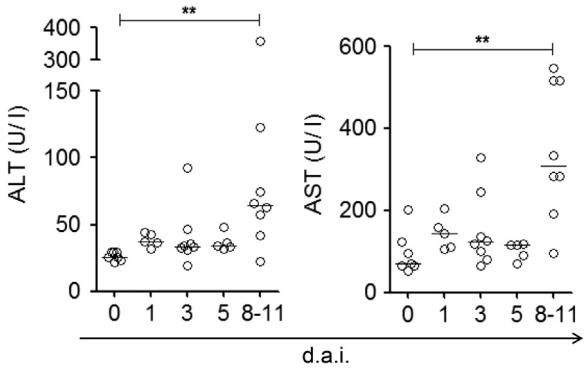

Fig. 11. Serum levels of liver enzymes in infected mice. The enzymes alanine aminotransferase (ALT) and aspartate aminotransferase (AST) were quantified by dry biochemistry at different days after infection (n ranging from 5 to 13). Statistical differences between non-infected and infected groups were evaluated using Mann–Whitney test ($^{**}p < 0.01$). d.a.i.-days after infection.

Discussion

The application of a neuroadapted dengue strain to generate a lethal infection after intracerebral inoculation in mice has been used since Sabin and Schlesinger (1945) and provides a very straightforward readout parameter for vaccine testing. The protective potential of a proposed vaccine or antiviral can be directly assessed by its capability or not to prevent morbidity and

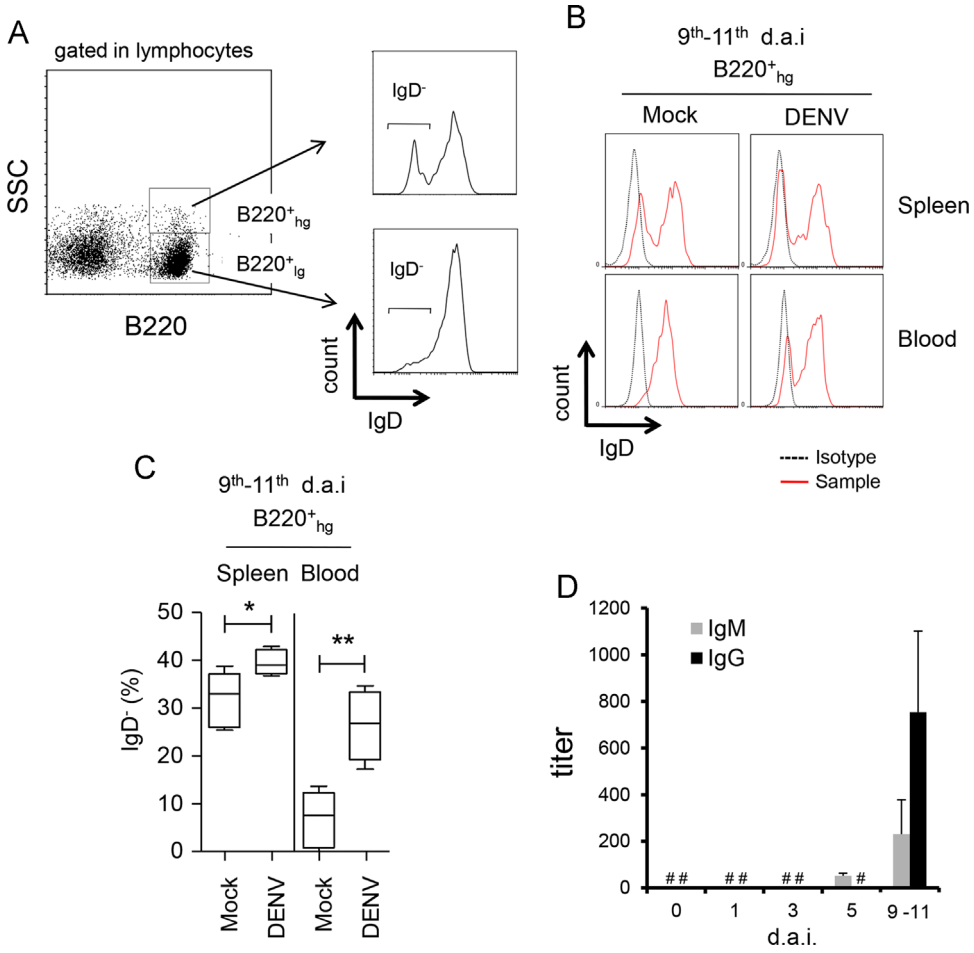

Fig. 12. Humoral immune response in infected BALB/c mice. B cell response was evaluated in blood samples of BALB/c mice intracerebrally inoculated with DENV2 in the period of 9–11 days after infection. (A) Flow cytometry strategy representing $B220^+$ cells analyzed in the lymphocyte region. The $B220^+$ lymphocytes were divided in events of high (hg) or low (lg) granulosity and the expression of IgD was measured in the cell surface. (B) Cytometric hystograms showing the expression profile of IgD and (C) the quantitative analysis of IgD^- cells gated in $B220^+_{hg}$ events present in spleen or blood samples of mice. Values represent percentages and statistical differences between non-infected and infected groups were evaluated using Mann–Whitney test ($^*p < 0.05$; $^{**}p < 0.01$). (D) Titer of anti-NS1 IgM and IgG measured by ELISA in plasma of mice at different d.a.i. Values are expressed as mean and standard deviation. Data represent a compilation of two independent experiments with groups of 5 animals in each test (total $n = 10$). d.a.i.-days after infection. #undetectable value.

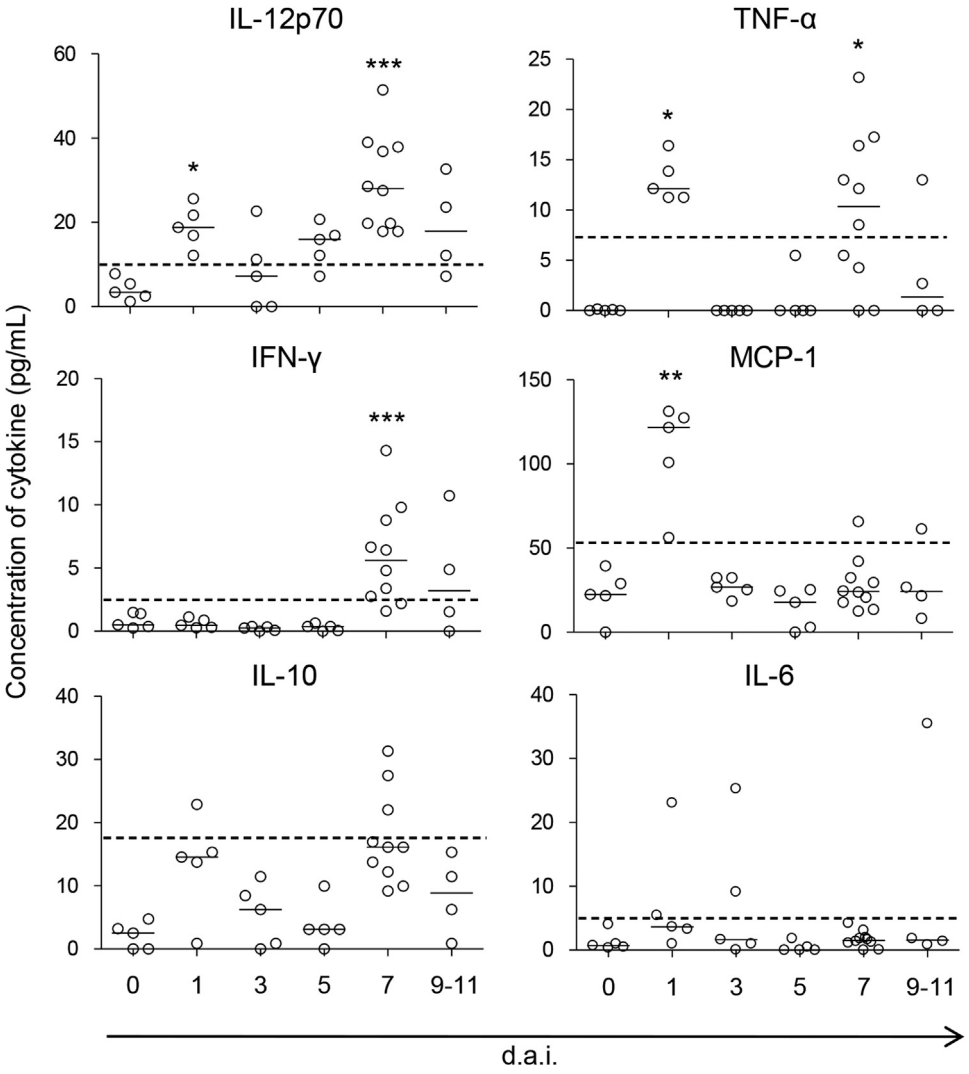

Fig. 13. Plasma levels of proinflammatory cytokines of infected mice. Plasma samples of BALB/c mice inoculated with DENV2 by the intracerebral route (*n* ranging from 4 to 10) were collected in different days post-infection and quantified for IL-12p70, TNF-α, IFN-γ, MCP-1, IL-10 and IL-6, using cytometric bead array technique. Values are plotted individually with median for each group. Statistical differences between non-infected and infected groups were evaluated using Mann–Whitney test (*$p < 0.05$; **$p < 0.01$). Dotted line represents the limit of detection for each cytokine defined by the manufacturer. d.a.i.-days after infection.

mortality among challenged animals. However, little is known about the systemic effects and the immune mechanisms involved during the virus infection. The present work was conducted in regards to better understand this mouse model. Under our experimental conditions, in which BALB/c mice received DENV2 NGC by the i.c. route, we found that usually at the 7th day of infection mice started to exhibit paralysis and hunchback posture, which are apparently the main symptoms within infected groups. After the appearance of this condition, the clinical signs generally evolved to death. Curiously, we observed that a fraction of infected mice succumbed to the infection differently, without showing any apparent CNS commitment. We hypothesized that distinct mechanisms of pathology and immunity, yet to be investigated, may lie behind such differences in morbidity in this inbred and isogenically-based animal model.

The first general discussion in this work is concerned on the typical clinical signs observed among infected mice. It is commonly discussed in the literature that the neurovirulence induced after DENV infection in mice would represent a major caveat in the determination of an appropriate model to study the disease (Yauch and Shresta, 2008; Sarathy et al., 2015). In fact, some authors defend that the involvement of CNS in DENV infections is not relevant in humans due to its rare occurrence (Patey et al., 1993; Lum et al., 1996). However, other reports showed that the CNS involvement with dengue actually is not so uncommon. From 150 fatal cases in Brazil (due to suspected infectious disease), 84 patients presented DENV in serum and 41 had the virus isolated from the cerebral spinal fluid (CSF) (Araújo et al., 2012). Studies in India also reported a relevant incidence of neurologic complications (2.6%) in infected patients (Koshy et al., 2012) and seizures (24%) in individuals with dengue encephalitis (Misra and Kalita, 2009). Although diagnostic criteria for dengue encephalitis have been proposed, they are controversial because detection of either viral RNA or specific IgM antibodies in the CSF may be disease-course dependent (Carod-Artal et al., 2013; Soares and Puccioni-Sohler, 2013). In consequence, this can eventually result in a wrong perception of the CNS involvement with dengue. In mouse models for dengue disease, paralysis is also observed even when using non-intracerebral infection routes or non-neuroadapted virus strains. For example, A/J mice, engrafted SCID mice and AG129 mice can exhibit paralysis after infection with DENV, in the last case after TNF-α inhibition (Lin et al., 1998; Shresta et al., 2004; Zellweger et al., 2013; Plummer and Shresta, 2014). Based on these observations, we may consider that the neuroadaptation of DENV

strains impacted mainly in the ability to induce lethality in immunocompetent mice, but the neurotropism of DENV in these animals seems to be a natural characteristic of this virus.

Initially, to investigate the intracerebrally infected animals, we measured the presence of infective virus particles in the brain and bloodstream. As expected, considerable amounts of virus were found in brain tissues collected in all time points (1 to 9–11 d.a.i.). Interestingly, the number of virus particles significantly decreased at the 5th d.a.i., after which it gradually increased until the end of the evaluation (9–11 d.a.i.). In addition to that, T cell infiltrates were found in the CNS (characterized by flow cytometry and histological analysis) of animals in late stages of infection (9–11 d.a.i.). Apart from other potential protective mechanisms in the CNS, the correlation between the increased virus titers in the brain in late stages of infection and the presence of T cell infiltrates in this organ suggested an ongoing peripheral cellular immune response. These results may contradict traditional theories, because the CNS is considered an immune-privileged tissue protected by a specific vessel structure, the blood–brain barrier (BBB), which in turn should block the migration of lymphocytes into this area. However, studies already demonstrated that upon infection or traumatic injury in the CNS, various immune cells are recruited to the affected space, trespassing the BBB (Arima et al., 2012; Kamimura et al., 2013). It is important to note that mock-inoculated animals, which also had the traumatic injury of injection, did not show tissue damages or cell infiltrates as observed in the brain of infected animals, thus reinforcing the direct effect of virus infection.

The spread of infective virus particles to the circulation in this animal model, although in a low magnitude, was also an important finding which can explain the systemic effects that we have observed. Consistent to this, T cell infiltrates and activated/effector T cell phenotypes in liver tissues of infected mice were also found. Taken together, these results suggested that the virus present in the circulation could affect peripheral organs. Other studies have also shown that the liver is an important target organ during DENV infection in mice. C57BL/6 mice infected intravenously (Sung et al., 2012) and BALB/c mice that received the virus by the subcutaneous (França et al., 2010), intraperitoneal (Paes et al., 2005) or intravenous (Paes et al. 2009) routes presented hepatic alterations. The major hepatic alterations observed in our study were steatosis, necrosis, areas of hemorrhage and edema/plasma leakage, which are similar to the effects described in fatal human cases (Bhamarapravati et al., 1967; Burke, 1968; Couvelard et al., 1999; Huerre et al., 2001; Basílio-de-Oliveira et al., 2005; Martina et al., 2009; Póvoa et al., 2014) as well as in other mouse models (Paes et al., 2005, 2009). Moreover, a significant increase of AST levels was detected in serum of infected mice at late stages of infection. In congruence to these findings, it was also reported that an increase of this liver enzyme occurs both in humans and mice due to dengue infection (Nguyen et al., 1997, Souza et al., 2004, Paes et al., 2005, 2009). Still considering our studied mouse model, diffuse mononuclear cell infiltrates in pia mater and in the molecular layer was found in the brain of infected mice. Perivascular leukocyte cell migration was also characterized in the temporal cortex. Similar findings were also seen in other reports of mouse models for dengue disease concerning different serotypes (Bordignon et al., 2008, Velandia-Romero et al., 2012, de Souza et al., 2013).

After the intracerebral infection of BALB/c mice, apart from the effects described above, we also found activated T cells in spleen and blood of these animals as well as humoral and cytokine responses. The participation of these responses is well documented in dengue cases (Rothman, 2011). One assumption that would explain the systemic involvement after the i.c.-infection, is that during inoculation, the mechanic damage would also result in virus spread to the circulation. This way, virus particles would infect other locations and antigens could reach lymphoid organs. Another possible explanation would be the commitment of the BBB due to the establishment of virus infection in the brain leading to virus spread. A third supposition to analyze this scenario involves a physiological communication between the CNS environment and the periphery. Classically, we understand that the relative immune privilege of the CNS is based upon a lack of access of cells and antigens from the brain to secondary lymphoid organs (Engelhardt and Coisne, 2011). Even though no classical lymph vessels are present in the CNS, several exit routes of the brain for cells and antigens are now well established (Weller et al., 2010; Laman and Weller, 2012). According to reports in the literature, it seems that due to an efficient drainage of both cerebrospinal fluid and interstitial fluid from the CNS, antigen presenting cells (APCs) and antigens existing in the brain tissue would reach regional lymphoid organs (Laman and Weller, 2012). It was found, for example, that in healthy animals dendritic cells injected into the CSF, migrate to cervical lymph nodes and may also build the connection to the humoral response, since these cells preferably migrate to B-cell regions in the lymphoid tissue (Hatterer et al., 2006). Thus, in the present mouse model, we speculate that a possible escape of APCs though specific exit routes present in the CNS would represent an important link between the i.c.-infection and the systemic effects observed. Yet, more investigation is still necessary in order to ensure the participation of these mechanisms in this model.

Taken together one important advantage of this murine model is the possibility to evaluate immune mechanisms elicited from an immunocompetent organism after challenge with DENV. Since no appropriate mouse model for dengue is yet available, the present work aimed to better understand the environment, effects and limitations of this still poorly described model that has been extensively used among the scientific community. Under our experimental conditions, infection in these animals led to systemic effects. Although the correlation of these systemic findings to the disease in humans has limitations due to the infection route and the used dengue virus variant, our data wide the knowledge about such model and highlights an interplay between the CNS commitment and peripheral effects.

Conclusions

In this work, we found that immunocompetent BALB/c mice inoculated by the i.c. route with a neuroadapted DENV strain can display peripheral effects such as cellular and humoral responses. These effects included: T cell activation and migration to affected organs, antibody production against virus proteins, and pro-inflammatory cytokine production. Besides lethality, these parameters may represent new endpoints to evaluate anti-dengue vaccines and/or antiviral substances. Even though the relevance of this murine model to describe dengue pathogenesis in humans may be restricted, this work provides a better understanding of such approach.

Materials and methods

Mice infection

The mouse–brain adapted dengue 2 virus (DENV2), strain New Guinea C (NGC) (GenBank M29095), was used for animal infections. DENV2 NGC strain propagation was carried out in Vero cells cultured in medium 199 with Earle salts (E199) buffered with sodium bicarbonate (Sigma, USA), supplemented with 10% fetal bovine serum (FBS, Invitrogen, USA). Supernatants obtained from cell cultures without virus were used for mock inoculations.

Experiments with mice were conducted in compliance with ethical principles in animal experimentation stated in the Brazilian College of Animal Experimentation and approved by the Institute's Animal Use Ethical Committee (approval ID: L067/08 and LW14/12).

Male BALB/c mice, specific pathogen free (SPF), 4 to 6 weeks old, were anesthetized with a mixture of ketamine–xylazine (Erhardt et al., 1984) and intracerebrally inoculated with 30 μL of DENV2 NGC 40 LD_{50}, diluted in E199 medium. For recording mortality rates, groups of animals were followed up for 21 days post infection and after that period they were sacrificed. Morbidity signs were count as the appearance of hind leg paralysis and alterations in spinal column. Infected or control animals were also sacrificed at different time points for kinetic studies, and blood, obtained from cardiac puncture, spleens, livers and brains were collected for further analysis.

Virus detection

Brain, liver and serum samples were obtained from animals inoculated with DENV2, or with mock control, at days 1, 3, 5, 7, and 9–11 after infection and stored in liquid nitrogen. DENV2 detection was performed in Vero cell monolayers grown in 24-well plates with medium E199, 1% garamycin, buffered with 5% sodium bicarbonate, supplemented with 5% FBS, and maintained at 37 °C in 5% CO_2. In the next day, brain or liver samples, macerated in E199 medium, as well as serum, were serially diluted (from 10^1 to 10^6) and added to cell monolayers, followed by incubation for 1 h at 37 °C in 5% CO_2. Culture medium was then removed and cells were maintained for 6 days with 1 ml of semi-solid E199 medium (with 3% carboxymethylcellulose, 1% garamycin, buffered with 5% sodium bicarbonate, supplemented with 5% FBS) also at 37 °C in 5% CO_2. After this period, cells were fixed with 10% formalin, stained with crystal violet and plaques were manually counted. When detection of DENV2 was in high magnitude, viral titers were calculated and expressed as the sample dilution which lead to the presence of 50% of plaque forming units (PFU)/mL and values were plotted as log10.

Immunohistochemistry assay

For immunohistochemistry assay paraffin-embedded liver tissues were cut (4 mm), deparaffinized in xylene and rehydrated with alcohol. Antigen retrieval was performed by heating the tissue in the presence of citrate buffer (Shi et al., 2011). The liver of mice were then blocked for endogenous peroxidase with 3% hydrogen peroxidase in methanol and rinsed in Tris–HCl (pH 7.4). Then, liver sections were incubated with Protein Blocker solution (Spring Biosciense) for 5 min at room temperature to reduce non-specific binding. Afterwards, samples were incubated over-night at 40 °C with anti-NS3 specific antibody (1:100) that recognizes recombinant dengue NS3 protein (expressed in *Escherichia coli* purified and produced in rabbit). In the next day, sections were incubated with anti-rabbit IgG, as secondary antibody-HRP conjugate (Spring Bioscience, CA, USA), for 30 min at room temperature. Mock-inoculated mice sections were used to control the reaction. Samples were revealed with diaminobenzidine (Dako, CA, USA) as a chromogen, sections were counter stained in Meyer's hematoxylin (Dako) and observed under an optical microscope.

Flow cytometry

For flow cytometry analysis, leukocytes were isolated from blood, spleen, brain and liver. All organs were dissociated in wire mesh screens using RPMI medium. Spleen macerates and blood samples were treated with BD FACS Lysing for red blood cell lysis and fixation according to manufacturer's instructions (BD Biosciences, USA). Brain infiltrated leukocytes were isolated by Percoll and Ficoll gradients. For the Percoll gradient, 5 mL of brain macerates were added to a tube containing 10 mL of RPMI, 9 mL of Percoll and 1 mL of PBS 10x. Samples were centrifuged at 7800 g for 30 min at room temperature. Leukocyte rings obtained after separation were washed and suspended in 5 mL of RPMI. Isolates were then gently transferred to tubes containing 5 mL of Ficoll. Samples were spinned down at 800 g for 30 min at room temperature. Mononuclear cell ring and interphase were isolated, washed two times and suspended in PBS pH 7.4. Samples were then treated with BD FACS Lysing solution. Leukocyte purification from liver macerates was carried out using only the Ficoll density gradient followed by treatment with BD FACS Lysing, as described above.

Isolated cells were finally washed and suspended in PBS/BSA 1%. Approximately 10^6 cells were stained on ice for 20 min in the dark with the following mab combinations: (i) B220-APC, IgD-FITC and CD4-PE; (ii) CD3-PE, CD4-Alexa Fluor 647, CD8-PercP and CD45RB-FITC or (iii) CD4-Alexa Fluor 647, CD8-PercP, CD45RB-FITC, CD44-PE and CD62L-PECy7. All mabs used for this work were obtained from BD Biosciences and background-staining controls were performed using isotypes recommended by the manufacturer. Samples were read in a BD FACS Canto II and analyzed offline with FlowJo (Three StarInc, USA) software.

Histological analysis

Brain and liver tissue samples from BALB/c mice inoculated with DENV2 NGC or mock were fragmented, fixed in formalin (10%) and blocked in paraffin resin. Sections were cut with 4 μm of thickness, deparafinized in xylene and rehydrated with alcohol, as previously described (Paes et al., 2009). Tissue sections were then stained with hematoxylin and eosin for histological examination and visualized under a Nikon ECLIPSE E600 microscope.

Hepatic enzyme quantification

BALB/c mice were bled on days 0, 1, 3, 5, 7 and 9–11 after virus inoculation and serum samples were stored at −70 °C until use. Levels of alanine aminotransferase (ALT) and aspartate aminotransferase (AST) were measured (U/L) by the biochemical analyzer Reflotron® Plus (Roche, Switzerland) as determined by the manufacturer.

Detection of anti-NS1 antibody response

Plasma samples were tested individually for the presence of NS1-specific antibodies by ELISA. Briefly, MaxiSorp plates (Nunc, Denmark) were coated with 0.4 μg/well of refolded recombinant NS1 protein (Amorim et al., 2010) in PBS, and incubated for 1 h at 37 °C. After this period, wells were overnight-blocked with 2% skim milk in 0.05% Tween-20-PBS (PBST). In the next day, serum samples were serially diluted and added to plates previously washed 5 times with PBST. After 1 h at 37 °C, plates were washed again with PBST and incubated with goat anti-mouse IgG or IgM, both conjugated with horseradish peroxidase (Southern Biotechnology, USA) for 1 h at 37 °C. Plates were washed in PBST and incubated with ortho-phenylenediamine dihydrochloride (Sigma, USA) and H_2O_2 for 20 min at room temperature. Reaction was stopped with 9 N H_2SO_4 solution and visualized at A 490 nm. Titers were established as the reciprocal of serum dilution that gave absorbance higher than mean values of respective non-infected mouse samples.

Cytokine quantification

Cytokines were measured with BD CBA Mouse inflammation kit (BD Bioscience) using plasma of infected animals. In this analysis, interleukin-12p70 (IL-12p70), interleukin-6 (IL-6), interferon-γ (IFN-γ), tumor necrosis factor-α (TNF-α), interleukin-10 (IL-10) and monocyte chemotactic protein 1 (MCP-1) were simultaneously detected in each sample. Detection was performed according to the manufacturer's instruction with modifications. Briefly, beads coated with six specific capture antibodies were pooled. Subsequently, 25 μL of the mixed captured beads, 25 μL of the tested plasma sample or the provided standard cytokines and 25 μL of PE-detection reagent were added consecutively to each assay tube, incubated for 2 h at room temperature in the dark. Samples were washed and centrifuged at 200 g for 5 min. Supernatants were discharged and the bead pellets were suspended in 300 μL of a buffer provided by the manufacturer. Samples were read on a BD FACS Canto II Flow Cytometer and analyzed by FCAP Array™ Software (BD Bioscience). Cytokine standards were serially diluted for the construction of calibration curves to assess cytokine concentrations in tested samples. The theoretical limits of detection were 10.7 pg/mL for IL-12p70, 5.0 pg/mL for IL-6, 2.5 pg/mL for IFN-γ, 7.3 pg/mL for TNF, 17.5 pg/mL for IL-10 and 52.7 pg/mL for MCP-1.

Statistical analysis

Data were analyzed with GraphPad prism software v 5.1 (La Jolla, USA) using non-parametric tests. Mann–Whitney test was applied for comparisons in ELISA or flow cytometry tests. Kaplan–Meyer survival distributions were evaluated using Log-Rank statistical test to check differences on biological treatments. Relevant differences were defined with probability (p) values inferior to 0.05.

Acknowledgments

We thank Dr. Luis Carlos S. Ferreira (Laboratory of Vaccine Development, Department of Microbiology, USP Brazil) for kindly supplying the recombinant NS1 protein, Dr. Ronaldo Borges (Federal University of Rio de Janeiro, Brazil) for providing the anti-NS3 specific antibody and Heloisa Diniz (Service of Image Production and Processing, IOC, Fiocruz, Brazil) for the technical assistance with the figures. Financial support: CNPq (44371/2014-0), FAPERJ (E26/110.271/2014), INCTV (573547/2008-4), PDTIS-FIOCRUZ (RVR11).

Appendix A. Supplementary material

Supplementary data associated with this article can be found in the online version at http://dx.doi.org/10.1016/j.virol.2015.12.006.

References

Amorim, J.H., Porchia, B.F., Balan, A., Cavalcante, R.C., da Costa, S.M., de Barcelos Alves, A.M., de Souza Ferreira, L.C., 2010. Refolded dengue virus type 2 NS1 protein expressed in Escherichia coli preserves structural and immunological properties of the native protein. J. Virol. Methods 167 (2), 186–192. http://dx.doi.org/10.1016/j.jviromet.2010.04.003.

Araújo, F.M., Araújo, M.S., Nogueira, R.M., Brilhante, R.S., Oliveira, D.N., Rocha, M.F., Cordeiro, R.A., Araújo, R.M., Sidrim, J.J., 2012. Central nervous system involvement in dengue: a study in fatal cases from a dengue endemic area. Neurology 78 (10), 736–742. http://dx.doi.org/10.1212/WNL.0b013e31824b94e9.

Arima, Y., Harada, M., Kamimura, D., Park, J.H., Kawano, F., Yull, F.E., Kawamoto, T., Iwakura, Y., Betz, U.A., Márquez, G., Blackwell, T.S., Ohira, Y., Hirano, T., Murakami, M., 2012. Regional neural activation defines a gateway for autoreactive T cells to cross the blood-brain barrier. Cell 148, 447–457. http://dx.doi.org/10.1016/j.cell.2012.01.022.

Azevedo, A.S., Yamamura, A.M., Freire, M.S., Trindade, G.F., Bonaldo, M., Galler, R., Alves, A.M., 2011. DNA vaccines against dengue virus type 2 based on truncate envelope protein or its domain III. PLoS One 6 (7), e20528. http://dx.doi.org/10.1371/journal.pone.0020528.

Basílio-de-Oliveira, C.A., Aguiar, G.R., Baldanza, M.S., Barth, O.M., Eyer-Silva, W.A., et al., 2005. Pathologic study of a fatal case of dengue-3 virus infection in Rio de Janeiro. J. Infect. Dis. 9, 341–347.

Berkowitz, A.L., Raibagkar, P., Pritt, B.S., Mateen, F.J., 2015. Neurologic manifestations of the neglected tropical diseases. J. Neurol. Sci. 349 (1–2), 20–32. http://dx.doi.org/10.1016/j.jns.2015.01.001.

Bhamarapravati, N., Tuchinda, P., Boonyapaknavik, V., 1967. Pathology of Thailand haemorrhagic fever: a study of 100 autopsy cases. Ann. Trop. Med. Parasitol. 61 (4), 500–510.

Bhatt, S., Gething, P.W., Brady, O.J., Messina, J.P., Farlow, A.W., Moyes, C.L., Drake, J.M., Brownstein, J.S., Hoen, A.G., Sankoh, O., Myers, M.F., George, D.B., Jaenisch, T., Wint, G.R., Simmons, C.P., Scott, T.W., Farrar, J.J., Hay, S.I., 2013. The global distribution and burden of dengue. Nature 496 (7446), 504–507. http://dx.doi.org/10.1038/nature12060.

Bordignon, J., Probst, C.M., Mosimann, A.L., Pavoni, D.P., Stella, V., Buck, G.A., Satproedprai, N., Fawcett, P., Zanata, S.M., de Noronha, L., Krieger, M.A., Duarte Dos Santos, C.N., 2008. Expression profile of interferon stimulated genes in central nervous system of mice infected with dengue virus type-1. Virology 377 (2), 319–329. http://dx.doi.org/10.1016/j.virol.2008.04.033.

Burke, T., 1978. Dengue haemorrhagic fever: a pathological study. Am. J. Trop. Med. Hyg. 62, 682–692.

Carod-Artal, F.J., Wichmann, O., Farrar, J., Gascón, J., 2013. Neurological complications of dengue virus infection. Lancet Neurol. 12 (9), 906–919. http://dx.doi.org/10.1016/S1474-4422(13)70150-9.

Chimelli, L., Hahn, M.D., Netto, M.B., Ramos, R.G., Dias, M., Gray, F., 1990. Dengue: neuropathological findings in 5 fatal cases from Brazil. Clin. Neuropathol. 9 (3), 157–162.

Chuansumrit, A., Chaiyaratana, W.2, 2014. Hemostatic derangement in dengue hemorrhagic fever. Thromb. Res. 133 (1), 10–16. http://dx.doi.org/10.1016/j.thromres.2013.09.028.

Clements, D.E., Coller, B.A., Lieberman, M.M., Ogata, S., Wang, G., Harada, K.E., Putnak, J.R., Ivy, J.M., McDonell, M., Bignami, G.S., Peters, I.D., Leung, J., Weeks-Levy, C., Nakano, E.T., Humphreys, T., 2010. Development of a recombinant tetravalent dengue virus vaccine: immunogenicity and efficacy studies in mice and monkeys. Vaccine 28 (15), 2705–2715. http://dx.doi.org/10.1016/j.vaccine.2010.01.022.

Costa, S.M., Yorio, A.P., Gonçalves, A.J., Vidale, M.M., Costa, E.C., Mohana-Borges, R., Motta, M.A., Freire, M.S., Alves, A.M., 2011. Induction of a protective response in mice by the dengue virus NS3 protein using DNA vaccines. PLoS One 6 (10), e25685. http://dx.doi.org/10.1371/journal.pone.0025685.

Couvelard, A., Marianneau, P., Bedel, C., Drouet, M.T., Vachon, F., et al., 1999. Report a fatal case of dengue infection with hepatitis: demonstration of dengue antigens in hepatocytes and liver apoptosis. Hum. Pathol. 30, 1106–1110.

de Souza, K.P., Silva, E.G., de Oliveira Rocha, E.S., Figueiredo, L.B., de Almeida-Leite, C.M., Arantes, R.M., de Assis Silva Gomes, J., Ferreira, G.P., de Oliveira, J.G., Kroon, E.G., Campos, M.A., 2013. Nitric oxide synthase expression correlates with death in an experimental mouse model of dengue with CNS involvement. Virol. J. 10, 267. http://dx.doi.org/10.1186/1743-422X-10-267.

Engelhardt, B., Coisne, C., 2011. Fluids and barriers of the CNS establish immune privilege by confining immune surveillance to a two-walled castle moat surrounding the CNS castle. Fluids Barriers CNS 8 (1), 4. http://dx.doi.org/10.1186/2045-8118-8-4.

Erhardt, W., Hebestedt, A., Aschenbrenner, G., Pichotka, B., Blümel, G., 1984. A comparative study with various anesthetics in mice (pentobarbitone, ketamine-xylazine, carfentanyl-etomidate. Res. Exp. Med. (Berl) 184 (3), 159–169.

França, R.F., Zucoloto, S., da Fonseca, B.A., 2010. A BALB/c mouse model shows that liver involvement in dengue disease is immune-mediated. Exp. Mol. Pathol. 89 (3), 321–326. http://dx.doi.org/10.1016/j.yexmp.2010.07.007.

Gubler, D.J., 2012. The economic burden of dengue. Am. J. Trop. Med. Hyg. 86 (5), 743–744. http://dx.doi.org/10.4269/ajtmh.2012.12-0157.

Hatterer, E., Davoust, N., Didier-Bazes, M., Vuaillat, C., Malcus, C., Belin, M.F., Nataf, S., 2006. How to drain without lymphatics? Dendritic cells migrate from the cerebrospinal fluid to the B-cell follicles of cervical lymph nodes. Blood 107, 806–812.

Huerre, M.R., Lan, N.T., Marianneau, P., Hue, N.B., Khun, H., et al., 2001. Liver histopathology and biological correlates in five cases of fatal dengue fever in Vietnamense children. Virchows Arch. 438, 107–115.

Huy, N.T., Van Giang, T., Thuy, D.H., Kikuchi, M., Hien, T.T., Zamora, J., Hirayama, K., 2013. Factors Associated with Dengue Shock Syndrome: A Systematic Review and Meta-Analysis. PLoS Negl. Trop. Dis. 7 (9), e2412. http://dx.doi.org/10.1371/journal.pntd.0002412.

Kamimura, D., Yamada, M., Harada, M., Sabharwal, L., Meng, J., Bando, H., Ogura, H., Atsumi, T., Arima, Y., Murakami, M., 2013. The gateway theory: bridging neural and immune interactions in the CNS. Front. Neurosci. 7, 204. http://dx.doi.org/10.3389/fnins.2013.00204.

Kho, L.K., Sumarmo, Wulur, H., Jahja, E.C., Gubler, D.J., 1981. Dengue hemorrhagic fever accompanied by encephalopathy in Jakarta. Southeast Asian J. Trop. Med. Public Health 12 (1), 83–86.

Koshy, J.M., Joseph, D.M., John, M., Mani, A., Malhotra, N., Abraham, G.M., Pandian, J., 2012. Spectrum of neurological manifestations in dengue virus infection in Northwest India. Trop. Doct. 42 (4), 191–194. http://dx.doi.org/10.1258/td.2012.120286.

Laman, J.D., Weller, R.O., 2012. Editorial: route by which monocytes leave the brain is revealed. J. Leukoc. Biol. 92 (1), 6–9. http://dx.doi.org/10.1189/jlb.0212110.
Lin, Y.L., Liao, C.L., Chen, L.K., Yeh, C.T., Liu, C.I., Ma, S.H., Huang, Y.Y., Huang, Y.L., Kao, C.L., King, C.C., 1998. Study of dengue virus infection in SCID mice engrafted with human K562 cells. J. Virol. 72 (12), 9729–9737.
Lum, L.C., Lam, S.K., Choy, Y.S., George, R., Harun, F., 1996. Dengue encephalitis: a true entity? Am. J. Trop. Med. Hyg. 54, 256–259.
Martina, B.E., Koraka, P., Osterhaus, A.D., 2009. Dengue virus pathogenesis: an integrated view. Clin. Microbiol. Rev. 22 (4), 564–581. http://dx.doi.org/10.1128/CMR.00035-09.
Miagostovich, M.P., Ramos, R.G., Nicol, A.F., Nogueira, R.M., Cuzzi-Maya, T., Oliveira, A.V., Marchevsky, R.S., Mesquita, R.P., Schtzamyr, H.G., 1997. Retrospective study on dengue fatal cases. Clin. Neuropathol. 16 (4), 204–208.
Misra, U.K., Kalita, J., 2009. Seizures in encephalitis: predictors and outcomes. Seizure 18 (8), 583–587. http://dx.doi.org/10.1016/j.seizure.2009.06.003.
Nguyen, T.L., Nguyen, T.H., Tieu, N.T., 1997. The impact of dengue haemorrhagic fever on liver function. Res. Virol. 148 (4), 273–277.
Paes, M.V., Lenzi, H.L., Nogueira, A.C., Nuovo, G.J., Pinhão, A.T., Mota, E.M., Basílio-de-Oliveira, C.A., Schatzmayr, H., Barth, O.M., Alves, A.M., 2009. Hepatic damage associated with dengue-2 virus replication in liver cells of BALB/c mice. Lab. Invest. 89 (10), 1140–1151. http://dx.doi.org/10.1038/labinvest.2009.83.
Paes, M.V., Pinhão, A.T., Barreto, D.F., Costa, S.M., Oliveira, M.P., Nogueira, A.C., Takiya, C.M., Farias-Filho, J.C., Schatzmayr, H.G., Alves, A.M., Barth, O.M., 2005. Liver injury and viremia in mice infected with dengue-2 virus. Virology 338 (2), 236–246.
Patey, O., Ollivaud, L., Breuil, J., Lafaix, C., 1993. Unusual neurologic manifestations occurring during dengue fever infection. Am. J. Trop. Med. Hyg. 48, 793–802.
Plummer, E.M., Shresta, S., 2014. Mouse models for dengue vaccine and antivirals. J. Immunol. Methods 410, 34–38. http://dx.doi.org/10.1016/j.jim.2014.01.001.
Porter, K.R., Kochel, T.J., Wu, S.J., Raviprakash, K., Phillips, I., Hayes, C.G., 1998. Protective efficacy of a dengue 2 DNA vaccine in mice and the effect of CpG immuno-stimulatory motifs on antibody responses. Arch. Virol. 143 (5), 997–1003.
Póvoa, T.F., Alves, A.M., Oliveira, C.A., Nuovo, G.J., Chagas, V.L., Paes, M.V., 2014. The pathology of severe dengue in multiple organs of human fatal cases: histopathology, ultrastructure and virus replication. PLoS One 9 (4), e83386. http://dx.doi.org/10.1371/journal.pone.0083386.
Rothman, A.L., 2011. Immunity to dengue virus: a tale of original antigenic sin and tropical cytokine storms. Nat. Rev. Immunol. 11 (8), 532–543. http://dx.doi.org/10.1038/nri3014.
Row, D., Weinstein, P., Murray-Smith, S., 1996. Dengue fever with encephalopathy in Australia. Am. J. Trop. Med. Hyg. 54 (3), 253–255.
Sabin, A.B., Schlesinger, R.W., 1945. Production of immunity to dengue with virus modified by propagation in mice. Science 101 (2634), 640–642.
Sarathy, V.V., White, M., Li, L., Gorder, S.R., Pyles, R.B., Campbell, G.A., Milligan, G.N., Bourne, N., Barrett, A.D., 2015. A lethal murine infection model for dengue virus 3 in AG129 mice deficient in type I and II interferon receptors leads to systemic disease. J. Virol. 89 (2), 1254–1266. http://dx.doi.org/10.1128/JVI.01320-14.
Shi, S.R., Shi, Y., Taylor, C.R., 2011. Antigen retrieval immunohistochemistry: review and future prospects in research and diagnosis over two decades. J. Histochem. Cytochem. 59 (1), 13–32. http://dx.doi.org/10.1369/jhc.2010.957191.
Shresta, S., Kyle, J.L., Robert Beatty, P., Harris, E., 2004. Early activation of natural killer and B cells in response to primary dengue virus infection in A/J mice. Virology 319 (2), 262–273.
Soares, C., Puccioni-Sohler, M., 2013. Diagnosis criteria of dengue encephalitis. Arq. Neuropsiquiatr. 72 (3), 263.
Souza, L.J., Alves, J.G., Nogueira, R.M., Gicovate Neto, C., Bastos, D.A., Siqueira, E.W., Souto Filho, J.T., Cezário Tde, A., Soares, C.E., Carneiro Rda, C., 2004. Aminotransferase changes and acute hepatitis in patients with dengue fever: analysis of 1,585 cases. Braz. J. Infect. Dis. 8 (2), 156–163.
Sumarmo, W.H., Jahja, E., Gubler, D.J., Suharyono, W., Sorensen, K., 1983. Clinical observations on virologically confirmed fatal dengue infections in Jakarta, Indonesia. Bull. World Health Organ. 61 (4), 693–701.
Sumarmo, W.H., Jahja, E., Gubler, D.J., Sutomenggolo, T.S., Saroso, J.S., 1978. Encephalopathy associated with dengue infection. Lancet 1 (8061), 449–450.
Sung, J.M., Lee, C.K., Wu-Hsieh, B.A., 2012. Intrahepatic infiltrating NK and CD8 T cells cause liver cell death in different phases of dengue virus infection. PLoS One 7 (9), e46292. http://dx.doi.org/10.1371/journal.pone.0046292.
Valdés, I., Bernardo, L., Gil, L., Pavón, A., Lazo, L., López, C., Romero, Y., Menendez, I., Falcón, V., Betancourt, L., Martín, J., Chinea, G., Silva, R., Guzmán, M.G., Guillén, G., Hermida, L., 2009. A novel fusion protein domain III-capsid from dengue-2 in a highly aggregated form induces a functional immune response and protection in mice. Virology 394 (2), 249–258. http://dx.doi.org/10.1016/j.virol.2009.08.029.
Velandia-Romero, M.L., Acosta-Losada, O., Castellanos, J.E., 2012. In vivo infection by a neuroinvasive neurovirulent dengue virus. J. Neurovirol. 18 (5), 374–387. http://dx.doi.org/10.1007/s13365-012-0117-y.
Weller, R.O., Galea, I., Carare, R.O., Minagar, A., 2010. Pathophysiology of the lymphatic drainage of the central nervous system: implications for pathogenesis and therapy of multiple sclerosis. Pathophysiology 17 (4), 295–306. http://dx.doi.org/10.1016/j.pathophys.2009.10.007.
World Health Organization, 2013. WHO Expert Committee on Biological Standardization. World Health Organ Tech Rep Ser, 979, 1–366 back cover.
Yauch, L.E., Shresta, S., 2008. Mouse models of dengue virus infection and disease. Antivir. Res. 80 (2), 87–93. http://dx.doi.org/10.1016/j.antiviral.2008.06.010.
Zellweger, R.M., Miller, R., Eddy, W.E., White, L.J., Johnston, R.E., Shresta, S., 2013. Role of humoral versus cellular responses induced by a protective dengue vaccine candidate. PLoS Pathog. 9 (10), e1003723. http://dx.doi.org/10.1371/journal.ppat.1003723.